Non-equilibrium Models for Two Phase Flow in Porous Media: the Occurrence of Saturation Overshoots

C.J. van Duijn[1], S.M. Hassanizadeh[2], I.S. Pop[1,*], P.A. Zegeling[2]

([1]Eindhoven Univesity of Technology, The Netherlands, [2]University of Utrecht, The Netherlands)

*Correspondence author: Dept. of Mathematics and Computer Science, Eindhoven University of Technology, PO Box 513, 5600 MB Eindhoven, The Netherlands
Fax: +31 40 2442489 Email: i.pop@tue.nl

Abstract
Several experiments have evidenced the occurrence of saturation overshoots for flows in homogeneous porous media. Such phenomena are ruled out by standard mathematical models, which are based on equilibrium assumptions. In this presentation we discuss non-equilibrium models, in particular including dynamic effects in the capillary pressure. This leads to extensions of the classical Buckley-Leverett (BL) equation, a commonly accepted model for two-phase flow in porous media. For this extended equation we investigate the existence of traveling wave solutions. Based on this we explain the occurrence of saturation overshoots, and discuss the profiles obtained for one phase or two phase flow models.

Introduction

Reliable mathematical models and simulation tools are essential for an optimal exploitation of geological resources. Thinking at processes like water flow in the subsurface, water driven oil recovery, or geological CO_2 storage (see [1], [12], or [17]), the mathematical models are conservation laws: nonlinear evolution equations having either a hyperbolic or a parabolic character, depending whether capillary effects are disregarded or not.

In this contribution we consider mathematical models at the Darcy scale, where differences between pores and the solid matrix, or interfaces between fluids in a particular pore are not taken into account. The main focus is on the effect of so-called non-equilibrium effects appearing in the constitutive relationships between quantities involved in the modelling. In particular, the saturation – phase pressure difference relationship is complemented by terms responsible for dynamic, non-equilibrium effects. Such mathematical models have been developed in [11] based on thermodynamic arguments. For alternative modeling approaches we refer to [5], [16], [18], where micro-scale interfaces between phases are taken into account, [13], where distinction is made between percolating and non-percolating phases, and [19] for a model combining dynamic and hysteretic effects.

The need for such models is justified by experimental results as in [2] or [6]. Striking in these results is the occurrence of non-monotonic saturation profiles during imbibition, as well as a non-monotonic dependency of the phase pressure difference on the saturation. Such features are ruled out by standard, equilibrium models.

In this contribution we discuss the influence of non-equilibrium effects on the solution profile for the resulting mathematical models. Based on the travelling wave analysis for the dimensionless setting, we present regimes where dynamic effects do impact on the solution profiles, or where these have no major influence. Finally we discuss how dynamic effects can explain the saturation overshoot.

Flow in Porous Media

We consider a homogeneous porous medium having a constant porosity φ, and a constant intrinsic permeability $\underline{\underline{K}}$. The vertical coordinate is z (oriented downwards) and g denotes the gravitational acceleration constant. Two fluid phases (wetting and nonwetting - indexed by w or n) are present in the medium. To include one phase flows, an inert nonwetting phase is also allowed. With α standing for either w or n, we follow [1], [12] and consider the mass balance and Darcy's laws for both phases

$$\varphi \frac{\partial S_\alpha}{\partial t} + \nabla \cdot \underline{v}_\alpha = 0, \quad \text{with} \quad \underline{v}_\alpha = -\underline{\underline{K}} \frac{k_{r\alpha}}{\mu_\alpha} \nabla(p_\alpha - \rho_\alpha g z).$$

Here S_α is the saturation of phase α, $\underline{v}_\alpha$ the Darcy velocity, μ_α the dynamic viscosity, ρ_α the density, and p_α the pressure. Furthermore, $k_{r\alpha}$ stands for the relative permeability of the phase. As obtained experimentally, $k_{r\alpha} = k_{r\alpha}(S_\alpha)$ is an increasing function of the corresponding phase saturation.

The experiments reported in [6] refer to water flow in a thin tube. The tube is assumed initially dry, and the flow is determined by gravity and capillary effects, as well by the injection of water encountered at the inlet of the tube. Since the tube is insulated, no normal flow is encountered at lateral walls. Combined with the homogeneity of the medium and since the initial saturation is constant, the experiment can be viewed as one-dimensional. Similarly, the experiments in [2] are carried out in a vertical column, but the lateral flow can be disregarded as well and the initial and inflow conditions are constant as well. This is why below we only focus on models in one spatial dimension.

We start by considering a one-phase flow model, which is related to the context in [6] by assuming that the air is a totally inert phase having constant pressure, but no influence on the water flow. Combining the Darcy law and the mass balance equation for water gives the Richards equation

$$\varphi \partial_t S_w - \partial_z (\underline{\underline{K}} \frac{k_{rw}}{\mu_w} (\partial_z p_w - \rho_w g \mathbf{e}_z)) = 0. \tag{1}$$

In this case, the capillary pressure is the opposite of the water pressure $P_c = -p_w$.

A two-phase flow model instead has to be taken into account to model the situation in [2]. Then, for $\alpha \in \{w, n\}$, the same steps lead to

$$\varphi \frac{\partial S_\alpha}{\partial t} - \partial_z \cdot \left(\underline{\underline{K}} \frac{k_{r\alpha}}{\mu_\alpha} (\partial_z p_\alpha - \rho_\alpha g \mathbf{e}_z) \right) = 0, \tag{2}$$

involving four unknowns (the saturations S_α and pressures p_α). In this case the system is closed by

$$S_w + S_o = 1, \text{ and } p_n - p_w = P_C,$$

with P_C being again the capillary pressure. This allows eliminating one saturation (e.g. S_n). By an abuse of notation, the nonwetting relative permeability become a decreasing function ofS_w,

$$k_{rn} = k_{rn}(1 - S_w) =: k_{rn}(S_w). \tag{3}$$

Working in one spatial dimension, and assuming that the inlet is not permeable for the air, whereas the water injection rate there is constant in time, the total velocity

$$\underline{q} = \underline{v}_w + \underline{v}_n \tag{4}$$

remains constant in both time and space. Having in mind the above, one can reduce the two-phase flow model to a scalar equation in S_w

$$\begin{aligned} \varphi\, \partial_t S_w + \partial_z \left(\underline{q} f(S_w) + \frac{\underline{\underline{K}}}{\mu_n} k_{rn}(S_w) f(S_w)(\rho_w - \rho_n) g \right) \\ + \partial_z \left(\frac{\underline{\underline{K}}}{\mu_n} k_{rn}(S_w) f(S_w)\, \partial_z P_C \right) = 0. \end{aligned} \tag{5}$$

The function f is the fractional flow function

$$f(S_w) = \frac{k_{rw}(S_w)}{k_{rw}(S_w) + M k_{rn}(S_w)}, \tag{6}$$

where $M = \mu_w/\mu_n$ is the mobility ratio of the two phases.

Equilibrium vs. non-Equilibrium Models

Either equations (2) or (5) are scalar, but involve two unknowns: the phase pressure difference P_c and the (wetting phase) saturation S_w. Based on experiments, a relation between P_c and S_w can be established. In a standard framework, this relation is obtained under equilibrium conditions [1], providing $P_c = P_c(S_w)$ as a decreasing function. This assumes that all measurements are carried out for times that are sufficient to allow a static distribution of the fluids inside pores.

On the other hand, experiments in [2] have shown that equilibrium models may not be valid. In this sense, measurements under non-equilibrium conditions (when fluids do not reach a steady state between measurements) have given P_c–$S_w$relations that differ from those under equilibrium conditions. Similarly, the experiments in [6] reveal non-monotonic saturation profiles, which are ruled out by equilibrium models. Specifically, for a low flux at the inflow and implicitly a low total velocity of the fluids in the column, the observed saturation profiles were monotone, as predicted also by the standard, equilibrium models. For higher fluxes instead, so-called "saturation overshoots" were encountered: at the infiltration front, the saturation values were higher than the ones at the influx. At even higher fluxes, this profile became more intriguing: a saturation plateau that is higher than the saturation at the inflow was separated by two fronts, an infiltration front and a drainage front.

Therefore we consider the model proposed in [11], which includes the time derivative of S_w in the model for the phase pressure difference,

$$P_C = -P_C^e(S_w) - \hat{\tau}\partial_t S_w, \tag{7}$$

where P_C^e is the negative of the capillary pressure - saturation function determined under equilibrium conditions, whereas the last term accounts for the dynamic effects. The quantity $\hat{\tau}$ is assumed here constant, but in general it might depend on S_w.

Dimensionless Models

To understand the importance played by the different terms, and in particular the one accounting for the non-equilibrium effects in (7), we consider reference quantities for bringing the model to a dimensionless form. These quantities will be the same for both one phase

model and the two-phase one, and therefore the resulting dimensionless numbers are similar. With

$$L, Q = \underline{q}, T, P_{\mathrm{d}}, \tau_{\mathrm{ref}} \tag{8}$$

as reference values for the length, velocity, time, pressure, and dynamic coefficient, recalling that in the one spatial dimension the intrinsic permeability reduces to a scalar $K = \underline{\underline{K}}$, define

$$\begin{gathered} s := S_w, \quad q := \underline{q}/Q, \quad \Delta\rho := \rho_w - \rho_n, \\ \hat{P}_C := P_d p_C(s), \quad \tau := \hat{t}/\tau_{\mathrm{ref}}, \end{gathered} \tag{9}$$

and the dimensionless numbers

$$P_e := \frac{TQ}{\Phi L}, \quad G_r := \frac{KgT\Delta\rho}{\mu_n \Phi L}, \quad C_a := \frac{KP_d T}{\mu_n \Phi L^2}, \quad D_y := \frac{\tau_{\mathrm{ref}} K}{\mu_n \Phi L^2}. \tag{10}$$

Note that s, as well as the functions p_C, k_{rw}, k_{rn} and f are dimensionless.

The values for the dimensionless quantities are determined by the experimental setup. For the one phase model, the density difference $\Delta\rho = \rho_w - \rho_n$ is replaced by the water density ρ_w. Moreover, having in mind the experiments in [6], in the one dimensional case the reference value Q will be taken as the water inflow velocity (at the inlet). Then defining a P_e number makes sense in the one-phase case too. For the ease of presentation, the reference time T is then chosen such that $P_e = 1$. Furthermore, taking

$$\tau_{\mathrm{ref}} := \frac{\Phi K P_d^2}{\mu_n Q^2} \tag{11}$$

gives $D_y = C_a^2$. We note that this particular choice has no influence on the results, but simplifies the writing and the analysis, in particular when considering the travelling wave approach below.

Following the steps above one can bring the models in (2) and (5) to dimensionless forms

$$\partial_t s + \frac{1}{M} G_r \, \partial_z k_{rw}(s) = \frac{1}{M} C_a \, \partial_z [k_{rw}(s) \, \partial_z (p_C(s) + C_a \tau \, \partial_t s)], \tag{12}$$

respectively

$$\partial_t s + \partial_z \big[f(s) \big(1 + G_r k_{rn}(s) \big) \big] = C_a \partial_z [k_{rn}(s) f(s) \partial_z (p_C(s) + C_a \tau \partial_t s)], \tag{13}$$

where f is given in (6). Typical choices are

$$k_{rw}(s) = s^{1+p}, \quad k_{rn}(s) = (1-s)^{1+q}, \quad p_C(s) = s^{\lambda}, \tag{14}$$

with some positive parameters $p, q, \lambda > 0$.

Travelling Waves

A step towards understanding the structure of the infiltration profiles is to consider travelling wave (TW) solutions. Such waves can explain the occurrence of non-monotonic, oscillatory-type profiles in the experimental results. Moreover, as will be seen below, the two-pase situation can explain well the special structure of saturation profiles obtained for high injection rates at the inlet.

Note that both models given before (one-phase and two-phase) have the same structure, namely

$$\frac{\partial s}{\partial t}+\frac{\partial F(s)}{\partial z}=C_a\frac{\partial}{\partial z}\left[H(s)\frac{\partial}{\partial z}\left(p_C(s)+C_a\tau\frac{\partial s}{\partial t}\right)\right], \tag{15}$$

with the nonlinear functions

$$F(s)=G_r k_{rw}(s) and H(s)=k_{rw}(s), \tag{16}$$

for one phase flows, whereas for two phases we have

$$F(s)=f(s)\big(1+G_r k_{rn}(s)\big), H(s)=k_{rn}(s)f(s). \tag{17}$$

The TW analysis for both models is similar, but lead to different results. As we will see bellow, in particular the two-phase case will provide special profiles, exhibiting a plateau value. This behavior is due to the particular shape (convex-concave) of the term F in the two-phase case.

A first step in explaining the occurrence of the non-monotonic saturation profiles in [6], or of the non-monotonic phase pressure difference – saturation results in [2] is to answer the following question: given two saturation values (states), a left (inflow) one s_- and a right (outflow/initial) one s_+, do TW connecting these states exist? In the affirmative case, the next step is to investigate the qualitative behavior of these waves, in particular their monotonicity.

TW are solutions having the form

$$s(t,x)=u(\eta), \quad \text{with} \quad \eta=\frac{x-Ct}{C_a}.$$

As mentioned, these connect a left (inflow) state s_- to a right (outflow) one s_+. Standard transformations imply that u solves

$$k_{rn}(u)f(u)(C\tau u''-p_C(u)')=C(u-s_+)-\big(F(u)-F(s_+)\big), \tag{18}$$

for all $\eta\in(-\infty,\infty)$, where $u(-\infty)=s_-$, $u(+\infty)=s_+$. The behavior at $\pm\infty$ gives

$$C=C(s_-,s_+)=(F(s_+)-F(s_-))/(s_+-s_-). \tag{19}$$

Note that (18) becomes degenerate (the factor multiplying the derivatives on the right is vanishing) for values of u where one of the two relative permeability curves k_{rn} and k_{rw} vanish. For the models appearing commonly in the literature, this represents the completely unsaturated regime ($u=0$) or the fully saturated one ($u=1$).

Recalling the experimental setup in [2], [6], here we restrict to the case $s_->s_+$. The existence of such waves is obtained by means of phase plane arguments. Essentially one has to find orbits in the plane $u-v$, where $v=u'$. These orbits solve the system

$$\begin{cases}u'=v,\\ v'=\frac{1}{C\tau}(p_C{}'(u)v+G(u)),\end{cases} \tag{2}$$

connecting the stationary points $(s_-,0)$ and $(s_+,0)$.

With C given in (19), here

$$G(u)=\frac{C(u-s_+)-(F(u)-F(s_+))}{k_{rn}(u)f(u)} \tag{21}$$

One phase flow

For the one phase model (12), F defined by (16) has a convex profile, and TW solutions are possible whenever $s_- > s_+$. This follows by standard phase plane arguments. Without attempting to be mathematically rigorous (we refer to [3], [9] for the details) the following behavior is expected.

A. In the case of equilibrium models ($\tau = 0$), the system (20) reduces to the equation (18). Then s_- is an unstable stationary point and s_+ a stable one. The TW are monotonically decreasing, so no saturation overshoots are encountered.

B. For the non-equilibrium model ($\tau > 0$) instead, the stationary point$(s_+, 0)$ is a saddle. For $(s_-, 0)$, this depends on τ: a τ_* exists such that $(s_-, 0)$ is a saddle if $\tau \in (0, \tau_*)$, and is an unstable spiral if $\tau > \tau_*$. Consequently, the TW is monotone in the former case, and becomes oscillatory in the latter situation.

This behavior is displayed in Figures 1-4, presenting the orbit as well as the saturation profile in the two situations mentioned above: $\tau < \tau_*$ and $\tau > \tau_*$. Note that the in the second situation the profile becomes non-monotone, featuring saturation overshoot.

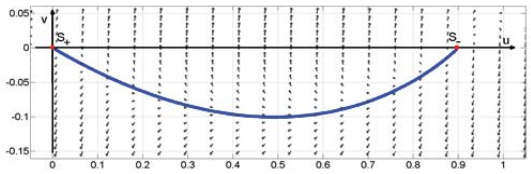

Figure 1. Orbit in the phase plane, $\tau < \tau_*$, one phase flow

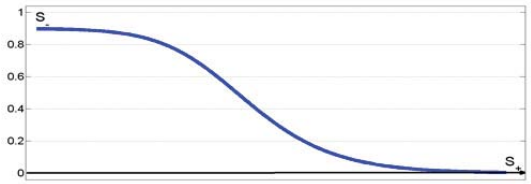

Figure 2. Water saturation profile, $\tau < \tau_*$, one phase flow

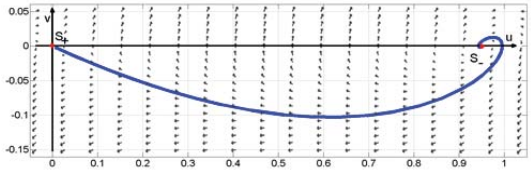

Figure 3. Orbit in the phase plane, $\tau > \tau_*$, one phase flow.

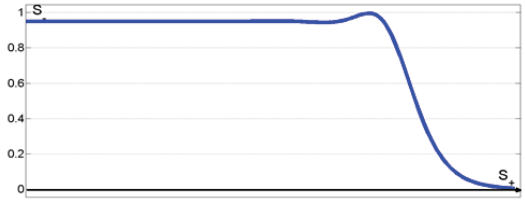

Figure 4. Water saturation profile, $\tau > \tau_*$, one phase flow

We mention that, regardless of the value of τ the wave connects s_- directly to s_+. In other words, no transition through some intermediate value is encountered, so no plateau value separated by an infiltration front and a drainage front can be obtained for the one-phase model.

Two-phase flow

The features of the two phase flow model are even richer than the single phase one. Recalling (13), the function F defined in (17) has alternating convex and concave regions. This situation is considered in [8] and [7], where for a fixed outflow value s_+, the dependency between τ and the inflow value s_- is analyzed. To present the results, we refer to Figure 5 below and assume that the right value s_+ is fixed. Then a coordinate α can be found where the tangent line through $(s_+, F(s_+))$ touches the graph of F.

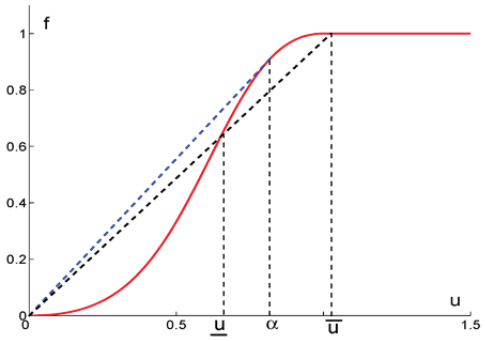

Figure 5. The points α, $\bar{u}(\tau)$ and $\underline{u}(\tau)$ for $\tau > \tau_*$.

A In the case of equilibrium models ($\tau = 0$), (18) is a first order equation. Then s_- is an unstable stationary point and s_+ a stable one. Then TW are only possible if $s_- \in (s_+, \alpha]$. Further the resulting waves are monotonically decreasing, eliminating saturation overshoots.

B If $\tau > 0$, as in the one-phase flow case a value τ_* exists such that if $\tau < \tau_*$, the dynamic effects do not influence the saturation profiles. Then these are completely similar to the ones provided by equilibrium models, and TW connecting any left state $s_- \in (s_+, \alpha]$ to s_+ are possible. Such waves are smooth and monotone, and no overshoot can be encountered (see Figures 6 and 7).

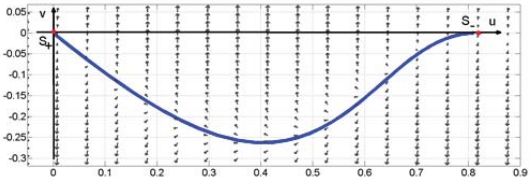

Figure 6. Orbit in the phase plane, $\tau < \tau_*$, two-phase flow

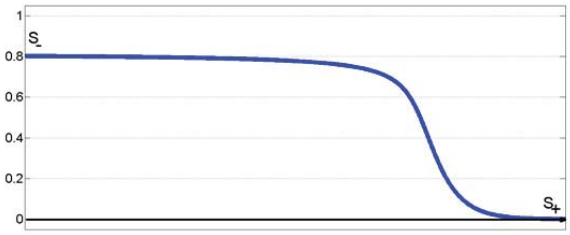

Figure 7. Water saturation profile, $\tau < \tau_*$, two phase flow

For the interesting case when $\tau > \tau_*$ we have:

- There exists a unique $\bar{u}(\tau) > \alpha$ that can be connected to s_+ through a monotone TW. The function $\bar{u}(\tau)$ is continuous and increasing (see Figure 8).

With $s_- = \bar{u}(\tau)$, the chord connecting $(s_-, F(s_-))$ and $(s_+, F(s_+))$ also intersects the graph of F in an intermediate point with u-coordinate $\underline{u}(\tau) \in (s_+, \alpha)$ (see Figure 5). Figure 8 presents the two branches, $\bar{u}(\tau)$ and $\underline{u}(\tau)$, which are computed numerically by a shooting scheme (see [7]).

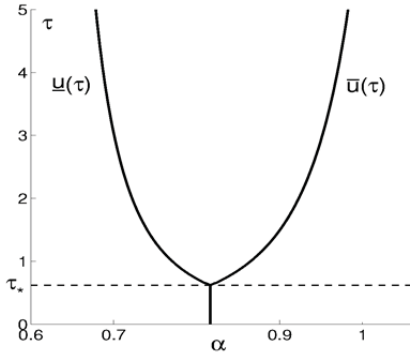

Figure 8. The branches $\bar{u}(\tau)$ (right) and $\underline{u}(\tau)$ (left), computed numerically (see [7])

In this situation we have:

- For each $s_- \in (s_+, \underline{u}(\tau)]$, there exists a TW connecting s_- tos_+.
- For each $s_- \in (\underline{u}(\tau), \bar{u}(\tau))$, no TW connecting s_- to s_+ exist.
- For each $s_- \in (\underline{u}(\tau), \bar{u}(\tau))$, TW connecting s_- to $\bar{u}(\tau)$ are possible.

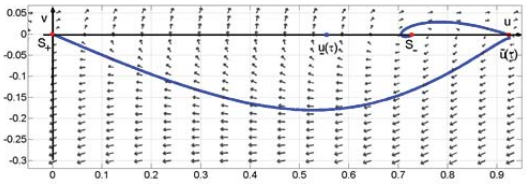

Figure 9 Orbits in the phase plane, $\tau > \tau_*$, $s_- \in (\underline{u}(\tau), \bar{u}(\tau))$, two-phase flow.

The stationary point $(s_-, 0)$in Figure 9 is an unstable spiral; $\left(\underline{u}(\tau), 0\right)$ and $(\bar{u}(\tau), 0)$ are saddle points. Two TW solutions are possible: one connecting $s_- \in \left(\underline{u}(\tau), \bar{u}(\tau)\right)$ to $\bar{u}(\tau)$ and one connecting $\bar{u}(\tau)$ to s_+. Since $(s_-, 0)$ is a spiral stationary point, the first wave is non-monotonic.

Numerical Solutions

Having understood the TW profiles occurring in the one- and two-phase flow models, we discuss the structure of the (numerical) solutions for the full models (12) and (13). In both cases we consider a finite but long one dimensional spatial interval $(0, L)$, start with $s(0, x) = s_+$ as initial condition and consider $s(t, 0) = s_-$ at the inflow and $\partial_x s(t, L) = 0$ at the outflow.

To emphasize on the effect of the dynamic terms, in both cases we only consider the situation $\tau > \tau_*$. We used different numerical schemes, analyzed in [4], [19], or [10] (see also [14] for a heterogeneous multi-scale method applicable to the hyperbolic limit where capillary effects are vanishing).

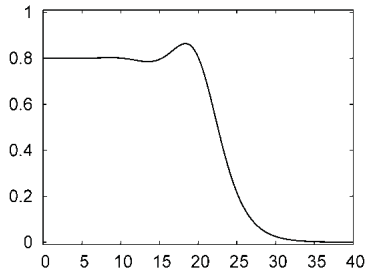

Figure 10. Non-monotonic solution, $\tau > \tau_*$, one phase

The solution in Figure 10 is computed for the one-phase model (12). As predicted by the phase plane analysis, it is non-monotonic featuring oscillations.

The numerical solution for the two-phase model (13), plotted in Figure 11, is more intriguing. Here one identifies two fronts, an infiltration one followed by a drainage front. The saturation between the two fronts reaches a “plateau value” that exceeds both inflow and initial saturations. The saturation overshoot is not only due to oscillations, but merely due to the plateau value.

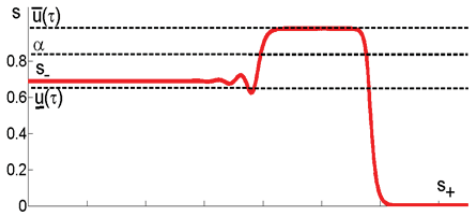

Figure 11. Non-monotonic solution, $\tau > \tau_*$, two phase

Referring to the phase plane analysis, the infiltration front is related to the saddle-saddle connection in Figure 9, whereas the drainage front is the spiral-saddle connection in the same figure. Moreover, the plateau value approximates (within the numerical accuracy) the value $\bar{u}(\tau)$ in the diagram presented in Figure 8.

Comparison to experiments

The TW analysis presented above can be related to the experimental results presented in [6], where non-monotonic infiltration profiles are observed, and [2], where a non-monotonic dependency between the saturation and the phase pressure difference has been measured. Such results are well explained by models including dynamic effects in the phase pressure difference for either one phase or two phase flows. The major difference between one and two phase flow models is in the behavior of the solution. Figure 10 displays a non-monotonic saturation profile obtained for (12). The solution there features oscillations behind the infiltration. For the two-phase model (13), two fronts are encountered: an infiltration front followed by a drainage one, with oscillations behind. The value between the two fronts rises significantly above the influx and the initial saturations.

In particular this latter feature respects very well the qualitative behavior reported in Figure 5 of [6]. There, as the influx is increasing, the saturation profile is changing from monotonic to oscillatory and up to the occurrence of two fronts separating a plateau value. Recalling (11), the water inflow velocity Q appears in the definition of τ_{ref}. Assuming that in the experimental setup the dimensional coefficient $\hat{\tau}$ is constant (in particular not depending on Q), the value of the dimensionless parameter τ (accounting for dynamic effects in the phase pressure difference can be identified as $\tau = \hat{\tau}/\tau_{ref}$. Therefore higher Q values imply an increase ofτ. This explains the occurrence of saturation overshoot for high inflow velocity values, and in particular the occurrence of plateaus in the saturation profiles obtained experimentally.

We conclude this part with the remark that one phase models can be seen as a limit case when the mobility ratio M in (6) vanishes or approaches infinity. Considering the air as a phase has important consequences for the saturation profile. This is due to the particular structure of the first order term in the model term, which is strictly convex for the one-phase model, and includes alternating convex and concave regions separated by inflection points in the two-phase model. In the former case, the non-equilibrium models can only provide non-monotonic waves, but no well-defined plateaus, as encountered in the latter case.

Conclusions

We have analyzed the saturation profile during infiltration in porous media. We compare the results for both two-phase and single phase flow. By means of travelling waves, we

discuss the profiles for standard, equilibrium models, as well as for non-equilibrium models when dynamic effects are included in the capillary pressure. We show that non-equilibrium effects are essential for explaining the occurrence
of saturation overshoots.

Acknowledgement

The authors are members of the International Research Training Group NUPUS funded by the German Research Foundation DFG (GRK 1398) and The Netherlands Organisation for Scientific Research NWO (DN 81-754). This work was also supported by the NWO cluster NDNS+ (http://www.ndns.nl/).

References

[1] J. Bear, Y. Bachmat, *Introduction to Modeling of Transport Phenomena in Porous media*, Kluwer Acad., Dordrecht, 1990.

[2] S. Bottero, S.M. Hassanizadeh, P.J. Kleingeld, T.J. Heimovara, *Nonequilibrium capillarity effects in two-phase flow through porous media at different scales*, Water Resour. Res. **47** (2011), W10505

[3] C. Cuesta, C.J. van Duijn, and J. Hulshof, *Infiltration in porous media with dynamic capillary pressure: Travelling waves*, European J. Appl. Math. **11** (2000), 381-397.

[4] C. Cuesta, I.S. Pop, *Numerical schemes for a pseudo-parabolic Burgers equation: Discontinuous data and long-time behaviour*, J. Comput. Appl. Math. **224** (2009), 269-283.

[5] L. Cueto-Felgueroso, R. Juanes, *Stability analysis of a phase-field model of gravity-driven unsaturated flow through porous media* Phys. Rev. E **79** (2009), 036301.

[6] D.A. DiCarlo, *Experimental measurements of saturation overshoot on infiltration*, Water Resour. Res. **40** (2004), W04215.

[7] C.J. van Duijn, Y. Fan, L.A. Peletier, I.S. Pop, *Travelling wave solutions for degenerate pseudo-parabolic equation modelling two-phase flow in porous media*, Nolinear Anal. Real World Appl. **14** (2013), 1361–1383.

[8] C.J. van Duijn, L.A. Peletier, I.S. Pop, *A new class of entropy solutions of the Buckley-Leverett equation*, SIAM J. Math. Anal. **39** (2007), 507–536.

[9] C.J. van Duijn, G.J.M. Pieters, P.A.C. Raats, *Steady flows in unsaturated soils are stable*, Transp. Porous Med. **21** (2004), 215-244.

[10] Y. Fan, I.S. Pop, *Equivalent formulations and numerical schemes for a class of pseudo-parabolic equations*, J. Comput. Appl. Math **246** (2013), 86-93.

[11] S.M. Hassanizadeh, W.G. Gray, *Thermodynamic basis of capillary pressure on porous media*, Water Resour. Res. **29** (1993), 3389–3405.

[12] R. Helmig, *Multiphase Flow and Transport Processes in the Subsurface*, Springer, 1997.

[13] R. Hilfer, F. Doster, P.A. Zegeling, *Nonmonotone Saturation Profiles for Hydrostatic Equilibrium in Homogeneous Porous Media*, Vadoze Z. Journal **11** (2012), doi: 10.2136/vzj2012.0021

[14] F. Kissling, R. Helmig, C. Rohde, *Simulation of Infiltration Processes in the Unsaturated Zone Using a Multi-Scale Approach*, Vadose Z. Journal 11 (2012), doi:10.2136/vzj2011.0193.

[15] S. Manthey, S.M. Hassanizadeh, R. Helmig, R. Hilfer, *Dimensional analysis of two-phase flow including a rate-dependent capillary pressure-saturation relationship*, Adv. Water Res. **31** (2008), 1137-1150.

[16] J. Niessner, S.M. Hassanizadeh, *A Model for Two-Phase Flow in Porous Media Including Fluid–Fluid Interfacial Area*, Water Resour. Res. **44** (2008), W08439, doi:10.1029/2007WR006721.

[17] J.M. Nordbotten, M.A. Celia, *Geological Storage of CO_2*, Wiley, New Jersey, 2012.

[18] I.S. Pop, C.J. van Duijn, J. Niessner, S.M. Hassanizadeh, *Horizontal redistribution of fluids in a porous medium: the role of interfacial area in modeling hysteresis*, Adv. Water Resour. **32** (2009), 383-390.

[19] A. Rätz, B. Schweizer, *Hysteresis models and gravity fingering in porous media*, Z. angew. Math. Mech.. (2012), doi: 10.1002/zamm.201200052